Microsyst Technol (2011) 17:971–981
DOI 10.1007/s00542-010-1220-8

TECHNICAL PAPER

Design of a hybrid optical image stabilization actuator to compensate for hand trembling

Choong Kim · Myeong-Gyu Song · No-Cheol Park · Kyoung-Su Park · Young-Pil Park · Douk-Young Song

Received: 31 August 2010 / Accepted: 31 December 2010 / Published online: 14 January 2011

Abstract In this paper, a novel hybrid optical image stabilization (OIS) actuator for digital camcorder is proposed. Image stabilization for this hybrid type consists of both radially and tangentially moving components to compensate for hand trembling. The proposed OIS actuator, which uses a voice coil motor method, is divided into two parts: a structure and a magnetic circuit. For the structural part, the driving mechanism consists of two systems: one system is based on a ball guide with a magnetic spring, and the other system is based on a pivot bearing. The former system is typically used as a driving mechanism in mobile devices, whereas the latter system has advantages such as mechanical stability and reduced friction. Overall, a magnetic spring between the magnet and yoke should be considered to select the best magnetic circuit part design and mechanism design. Regarding the electro-magnetic (EM) circuit, two types of EM circuits were designed to satisfy each direction: one circuit is a moving magnet circuit for the radial direction, and the other circuit is a moving coil for the tangential direction. In a digital camcorder, the space for the OIS actuator is limited, and thus, optimized actuator with adequate performances is required. To solve these problems, a sensitivity analysis was performed using the design of experiment procedure. Based on these results, an objective function was defined for the optimization procedure. Finally, the actuator was fabricated, and the dynamic characteristics and feasibility of adapting two types of mechanisms of the suggested OIS actuator were verified. The experimental results indicate that the proposed OIS actuator exhibits sufficient performance for the sensitivity.

C. Kim · M.-G. Song
Center for Information Storage Device, Yonsei University, Seoul, South Korea
e-mail: jumulri@yonsei.ac.kr

M.-G. Song
e-mail: netmang@yonsei.ac.kr

N.-C. Park (✉) · K.-S. Park · Y.-P. Park
Department of Mechanical Engineering, Yonsei University, Seoul, South Korea
e-mail: pnch@yonsei.ac.kr
URL: http://optomecha.yonsei.ac.kr/index.html

K.-S. Park
e-mail: pks6348@yonsei.ac.kr

Y.-P. Park
e-mail: park2814@yonsei.ac.kr
URL: http://vibcon.yonsei.ac.kr/

D.-Y. Song
Digital Media Business, Samsung Electronics Co., Ltd., Seoul, South Korea
e-mail: dy1.song@samsung.com

1 Introduction

Many studies have been performed regarding image stabilization (IS) systems to compensate for hand trembling in digital cameras, digital camcorders, and hybrid devices. Representative methods for IS systems include electric image stabilization (EIS), digital image stabilization (DIS), and optical image stabilization (OIS). Toshiro et al. (1990) studied EIS systems, Ko et al. (1998) studied DIS systems, and Koichi et al. (1993) studied OIS systems. Although EIS exhibit good performance, they have a high cost because gyroscopes or accelerometers are required, whereas DIS systems do not require these types of devices. However, DIS systems have a disadvantage that involves the limitation of compensation performance. The OIS systems compensate a blurred image by modifying the optical path

against hand trembling. To move the optical components, various methods such as voice coil motor (VCM) and piezo-electric (PZT) methods have been studied. Kauhanen and Rouvinen (2006) studied the PZT bimorph bending actuator, and Yu et al. (2005) studied the design of the VCM as a driving actuator. Although the PZT type has fast response characteristics, it requires a high voltage and has a high cost. However, the VCM type does not require high voltage to be applied for a fast response. Recently, the OIS actuator, which uses the VCM type, is being highlighted as a means to reduce motion blur because of its mechanical stability, low cost, and reliability. Also, the VCM actuator has advantages such as easy fabrication and fine motion. The driving mechanisms of the OIS actuator include the prismatic joint, ball guide, and compliant system. Song et al. (2009–2010) researched the OIS actuator in a cellular phone that uses a prismatic joint and a compliant mechanism for mechanical movement. However, this actuator has difficulties with mechanical stability and friction. Likewise, the conventional OIS actuator for digital camcorder had problems of mechanical stability, low sensitivity, and friction. In this paper, a novel hybrid OIS actuator is proposed to solve these problems; it has various advantages such as mechanical stability, no friction and good efficiency regarding its power consumption. For the electromagnetic (EM) circuit, two types of EM circuits were designed to satisfy each direction. One circuit is a moving magnet (MM) circuit for the radial direction, and the other circuit is a moving coil (MC) circuit for the tangential direction. For the structural part, the driving mechanism consists of two systems: one system is the ball guide method with a magnetic spring, and the other system is a pivot bearing. In a digital camcorder, the space for the OIS actuator is limited, and thus, optimized actuator with adequate performances is required. The design of experiment (DOE) procedure for the sensitivity analysis was performed to improve the driving performance of the actuator. Finally, the proposed actuator was fabricated, and the performance of the OIS actuator and feasibility of adapting a hybrid mechanism were experimentally verified.

2 Initial design

2.1 Mechanism design

Mechanisms for the moving part are divided into three types: prismatic joint, ball guide and compliant type, as shown in Fig. 1. Each mechanism has advantages and disadvantages. Even though the prismatic joint type has the advantage of the mechanical stability, it should overcome the disadvantage of friction problem. On the other hand, the compliant type has both merit of friction problem and demerit of mechanical stability. The ball guide type is better than the prismatic joint for the friction problem and is worse than the compliant type for the mechanical stability. To select the moving mechanism, both friction and mechanical stability should be considered in the structural design. Therefore, the hybrid type, which combines two mechanisms, is proposed as a new mechanism to improve performance. The prismatic joint type is not considered for the hybrid type due to a bad friction condition. Wire suspension as a compliant mechanism and ball bearing types are considered for the new mechanism. Wire suspension as a compliant mechanism is replaced with the pivot bearing to obtain improved stability and non-friction. This mechanism exhibits good efficiency with respect to power consumption due to its structural design. However, a magnetic spring is required in the design to meet the desired performance. Initially, it is necessary to define the specifications of the OIS actuator. In a study by Golik (2006), the amplitude for the handshake of a mobile device was measured with a laser pointer. Song et al. (2009) then used this method to define specifications. Kauhanen and Rouvinen (2006) reported that the handshake of a mobile device was 1.7° and 0–30 Hz. Choi et al. (2008) reported that the stroke of the actuator is dependent on the optical imaging system. A drive integrated circuit was considered, which is used in the OIS actuator, and the desired specifications of the OIS actuator and the performance of the conventional actuator are summarized in Table 1. The most prominent factors for designing the OIS actuator are

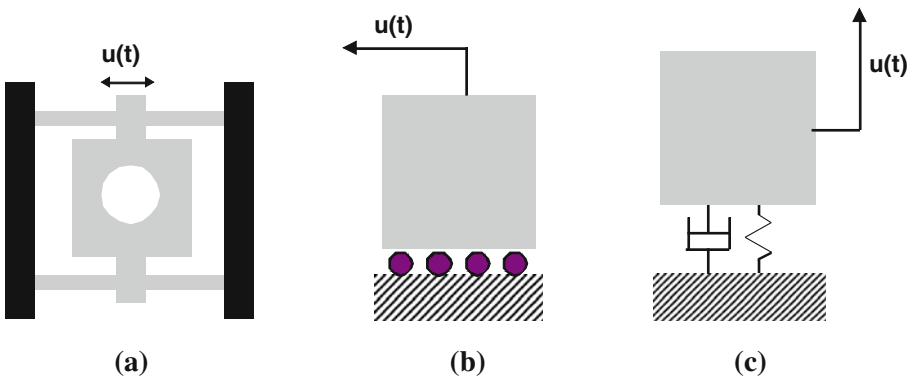

Fig. 1 Moving mechanism **a** prismatic joint, **b** ball guide and **c** compliant system

Table 1 Specifications of the OIS actuator

	Conventional	Desired
1st frequency (Hz)	31	30 ± 5
DC sensitivity (mm/V)	0.1	0.4
AC sensitivity (G/V)	1.0	1.2

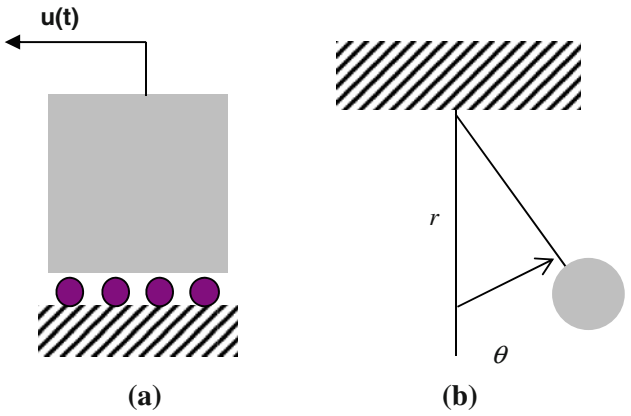

Fig. 2 Design concept for the moving mechanism **a** ball guide and **b** pivot bearing

the conceptual design and the specifications, which determine the final performance of the actuator. The proposed design concept, which uses a hybrid mechanism, is shown in Fig. 2. The initial model and moving mechanism, as shown in Figs. 3 and 4, were also designed after adopting the conceptual design. Mechanisms for each direction can be expressed, as shown in Eqs. 1 and 2, for the radial and tangential directions.

$$m\ddot{x} + c_1\dot{x} + kx = F_1 = S_1V_1 \tag{1}$$

where m is the mass, c_1 is the damping coefficient, k is the stiffness, F_1 is the driving force, S_1 is the sensitivity, and V_1 is the input voltage.

$$J\ddot{\theta} + c_2\dot{\theta} = F_2 \times r = T = S_2V_2 \tag{2}$$

where J is the moment of inertia, c_2 is the damping coefficient, F_2 is the driving force, r is the distance from the pivot to the center of the force, T is the torque, S_2 is the sensitivity, and V_2 is the input voltage.

2.2 Electromagnetic circuit design

In general, magnetic circuit parts, which consist of a magnet, coil and yoke, are divided into a moving coil type and a moving magnet type. These magnetic circuit parts have advantages and disadvantages. For a moving magnet type, not only the electromagnetic components but also the mechanical components should be considered. The driving force of electromagnetic components, which is shown in

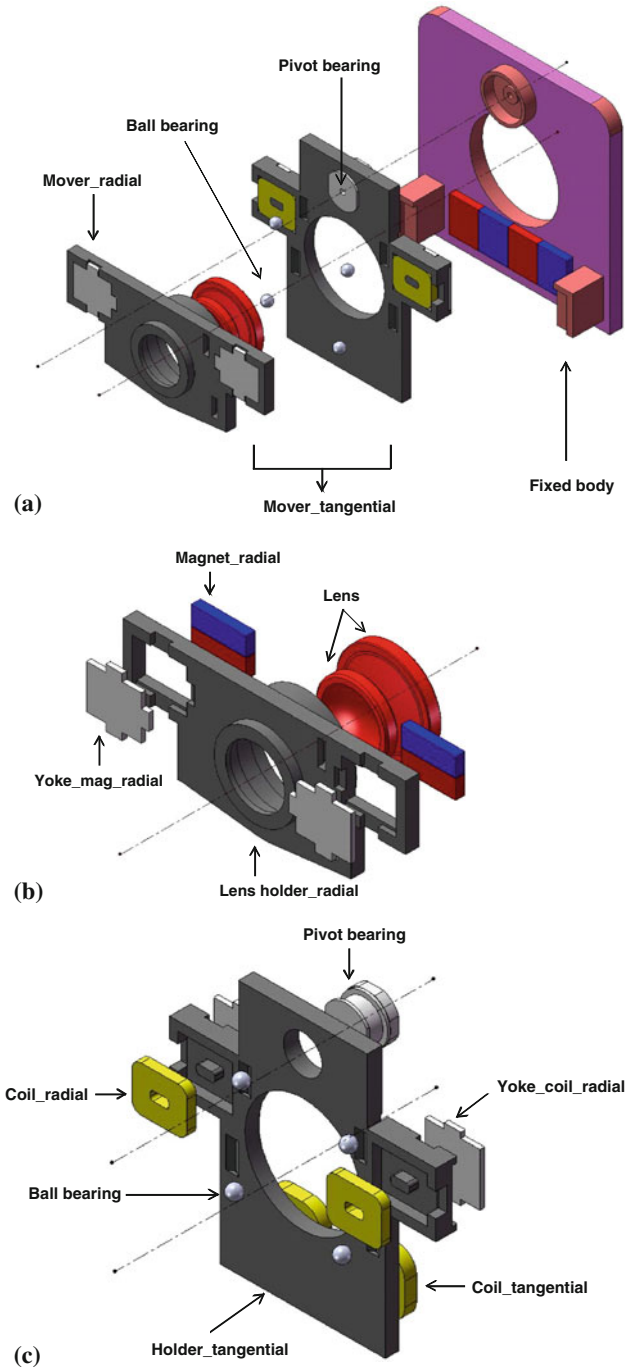

Fig. 3 Initial model **a** overall structure, **b** structure for the radial direction and **c** structure for the tangential direction

Eq. 3 as F_d, can be expressed by the mechanical components in Eqs. 1 or 2 as F_1 or F_2, respectively. For a moving coil type, the interruption between the coil connection and moving range should be verified. Additionally, an advantage of the moving mass is that the mass of the moving coil type is lower than the mass of the moving magnet type.

Chiu et al. (2007) used the following formulation for electromagnetic force

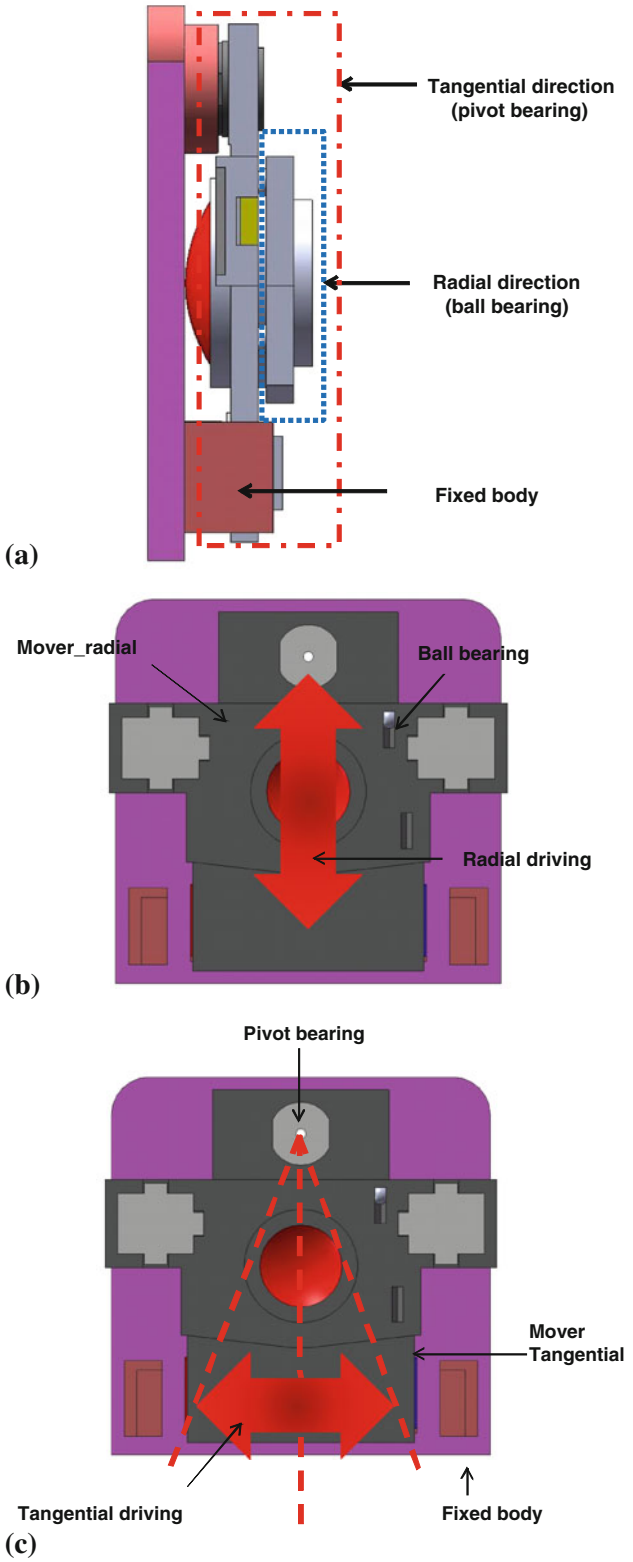

Fig. 4 Moving mechanism **a** side view of the overall mechanism, **b** mechanism for the radial direction and **c** mechanism for the tangential direction

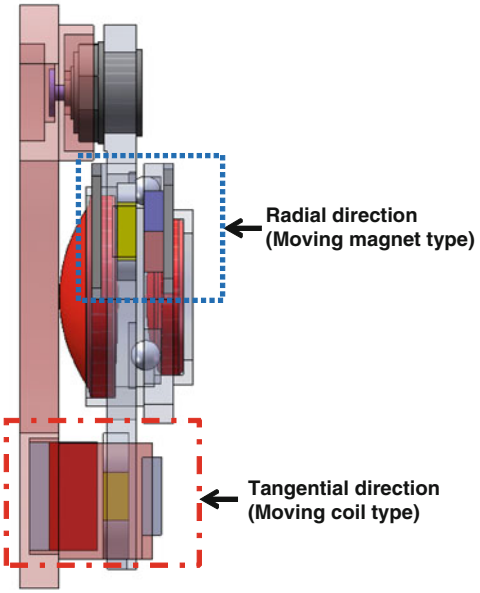

Fig. 5 Initial magnetic circuits

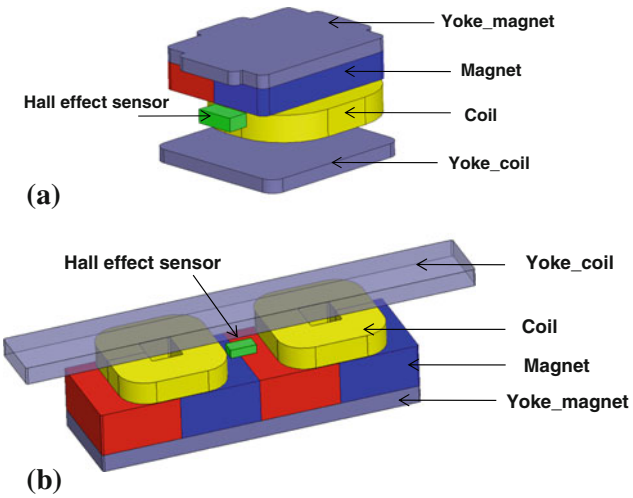

Fig. 6 Detail of the magnetic circuits **a** radial direction and **b** tangential direction

$$F_d = N \cdot i \cdot l_e \cdot B = N \cdot \frac{VA}{\rho L} \cdot l_e \cdot B \tag{3}$$

where F_d is the driving force, N is the number of coil turns, i is the amount of current applied to the voice coil, l_e is the effective length of the voice coil, B is the magnetic flux density, and V, A, ρ, and L are the applied voltage, cross-sectional area, electric conductivity, and total length of the coil, respectively. Based on the structural design and Eq. 3, the initial magnetic circuits were designed, as shown in Fig. 5.

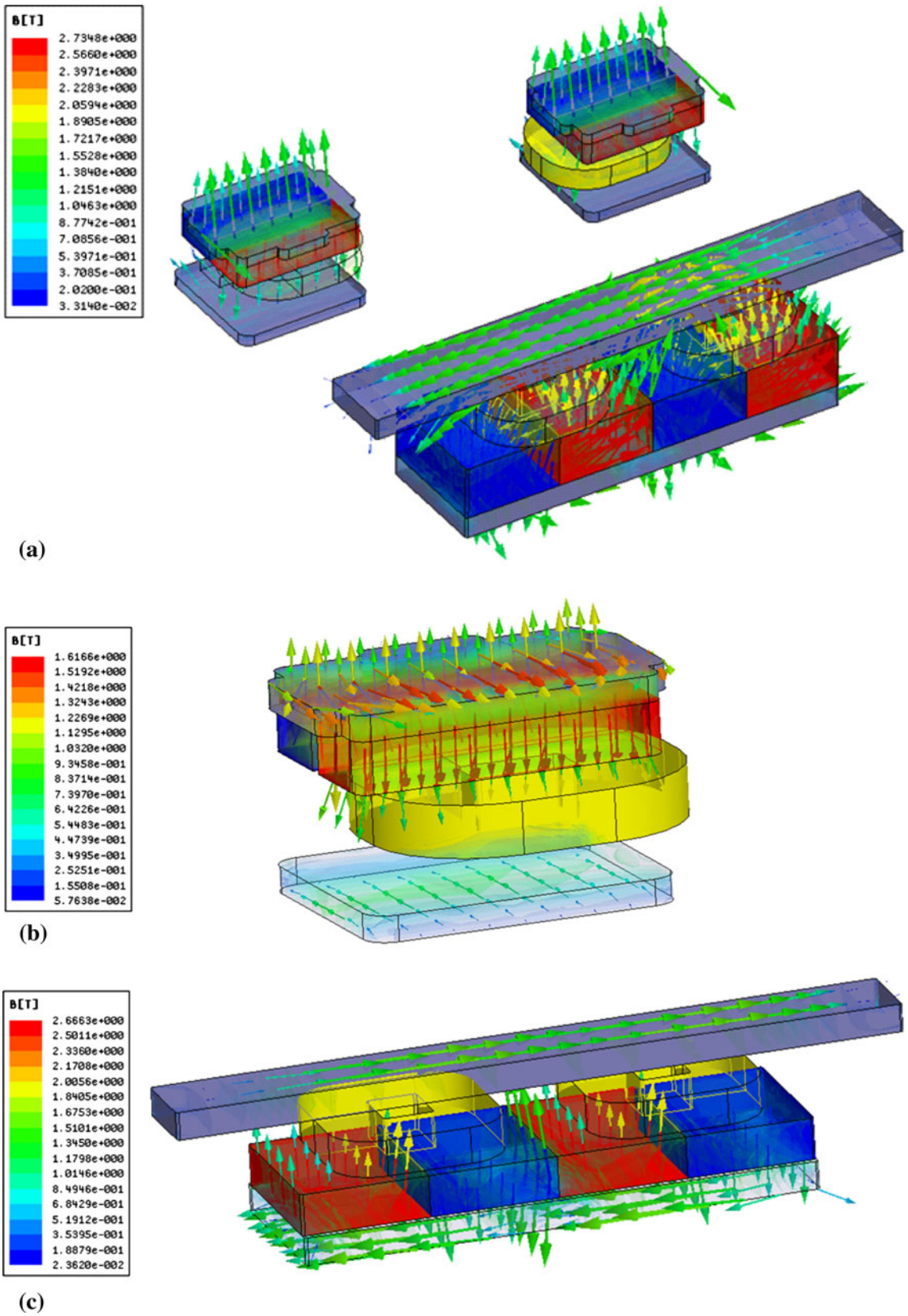

Fig. 7 Simulation results of magnetic flux density and magnetic intensity **a** overall magnetic circuit, **b** radial direction and **c** tangential direction

The detailed magnetic circuits for the radial and tangential directions are shown in Fig. 6. For the radial direction, the proposed magnetic circuits consisted of two magnets, four magnet yokes, two coils and Hall-effect sensor. And, for the tangential direction, the proposed magnetic circuits consisted of one magnet, two yokes, and two coils. The moving magnet type was selected for radial driving, and the moving coil type was selected for tangential driving. As stated above section, the hybrid mechanism, which uses both ball guide type and pivot bearing type, is proposed as a new mechanism. For the radial driving, the moving magnet type of ball guide mechanism is needed to use magnetic spring between magnet and yoke. And the structure of moving part is simple. For the tangential driving, the moving coil type of pivot bearing is required to make a simple connection of winding coils in one component. It is possible for the moving coil type not to consider the attraction force between magnet and yoke. The coils for radial and tangential driving can be placed in one component, as shown in Figs. 3 and 5. The Hall-effect sensor was used to detect the position of moving parts. To correct the position of moving parts, the linearity of the Hall-effect sensor should be verified.

2.3 Finite element analysis

The commercial software Maxwell 3D was used to simulate the driving force and magnetic flux. The magneto-static analysis was performed to consider the electromagnetic field effect on both sensors and error/noise. Figure 7 shows the simulation results of the magnetic flux and intensity. In detail, the electromagnetic field effect between two Hall-effect sensors has no effect on each other as shown in Fig. 7a. The magnetic flux density and intensity were not affected by each magnetic circuit. Song et al. (2010a, b) discussed the concept of a magnetic spring, preload and the linearity of the Hall-effect sensor. By using this concept, the magnetic spring and linearity of the Hall-effect sensor for each direction was simulated. Tables 2 and 3 show the design values of the initial magnetic circuit and coil specifications. Figure 8 shows the linearity of the Hall-effect sensor in each direction. The linearity of the Hall-effect sensor was verified within the moving

Table 2 Design values for the initial magnetic circuit

Variables (mm)	Radial direction				Tangential direction			
	X	Y	Z	T	X	Y	Z	T
Magnet	4.8	6.0	1.1		18.4	5.6	2.5	
Yoke_mag	5.0	6.0	0.5		18.4	5.3	1.0	
Yoke_coil	6.0	6.0	0.5		26.0	4.0	1.0	
Coil	5.0	6.0	1.0	2.0	6.5	6.2	1.3	2.2

Table 3 Coil specifications

Coil	Radial	Tangential
Diameter (mm)	0.083	0.094
Resistance (ohm)	31.77	30.22
Turns (number)	288	299
Current (A)	9.07	9.89

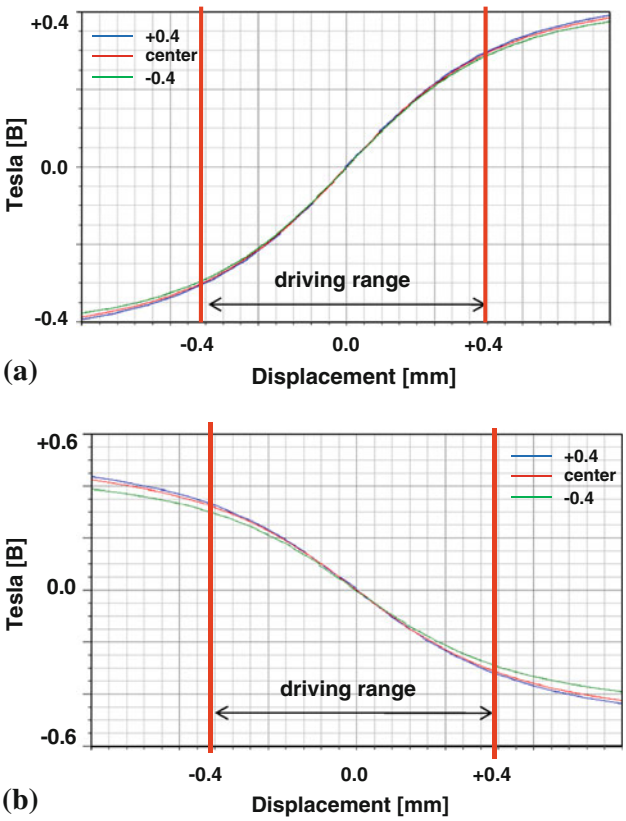

Fig. 8 Linearity of the Hall-effect sensor **a** radial direction and **b** tangential direction

Table 4 Performance of the initial model

	Desired	Initial	
		Radial direction (MM type)	Tangential direction (MC type)
1st frequency (Hz)	30 ± 5	39.5	–
Magnetic spring (N/m)	65 ± 20	107.5	–
DC sensitivity (mm/V)	0.4	0.35	–
AC sensitivity (G/V)	1.2	2.17	1.89

range [−0.4 mm to +0.4 mm]. The results from the simulation for the initial model are summarized in Table 4. For tangential driving, the AC sensitivity exhibits sufficient performance, and the linearity of the Hall-effect sensor is about 96% within the driving range. For radial driving, the DC sensitivity, magnetic spring and first frequency are not close to the target value, the AC sensitivity exhibits sufficient performance, and the linearity of the Hall-effect sensor is about 97% within the driving range. Therefore, the optimization is required for the magnetic spring, first frequency, and the DC sensitivity.

3 Optimized design

Electromagnetic circuit designs for each direction were determined in the previous section. The design variables were selected after considering the effect on the sensitivity and structural constraints. For the radial direction, Fig. 9a shows the design variables for the magnetic circuit that were used to perform the sensitivity analysis. The level of sensitivity analysis and range are shown in Table 5. The size of the magnet is very sensitive to the driving force, and the magnetic spring and first frequency exhibit similar behavior, as shown in Fig. 10. Therefore, the size of the yoke should be selected after considering the interaction among the design variables. Based on the sensitivity analysis, the objective function is defined as Eq. 4 for the radial direction, and the first frequency and normal force, which operates as an attractive force between the magnet and the yoke, are selected as constraints.

$$\begin{aligned} &\text{Minimize}\sqrt{\left(k_{t,i}-k_{t,desired}\right)^2} \\ &subject\ to\ k_{t,desired}=(2\pi f_o)^2 m \\ &f_o=30\pm 5\,\text{Hz}, \end{aligned} \tag{4}$$

where $k_{t,i}$ is the magnetic spring for the magneto-static simulation during iteration, $k_{t,desired}$ is the numerical value of the magnetic spring, f_0 is the first frequency, and m is the mass of the mover.

Constraint #1
26 (gf) ≤ normal force ≤ 36 (gf)
Constraint #2
25 (Hz) ≤ 1st frequency ≤ 35 (Hz)

The magnetic spring is associated with the Lorentz and reaction forces. Equations 5 and 6 describe the relationship between force and displacement and the magnetic spring for the optimized model. Figure 11 shows the Lorentz and reaction forces of the initial and optimized models.

$$F_{driving}=-F_{Lorentz}-F_{reaction} \tag{5}$$

$$k_t=\frac{F_{driving}}{y}=\frac{59.46(\text{mN})}{0.8\ (\text{mm})}=74.3\ (\text{N/m}) \tag{6}$$

For the tangential direction, the circuit exhibits a sufficient performance because the driving mechanism is free of friction. However, the performance can be improved by using the sensitivity analysis. Figure 9b

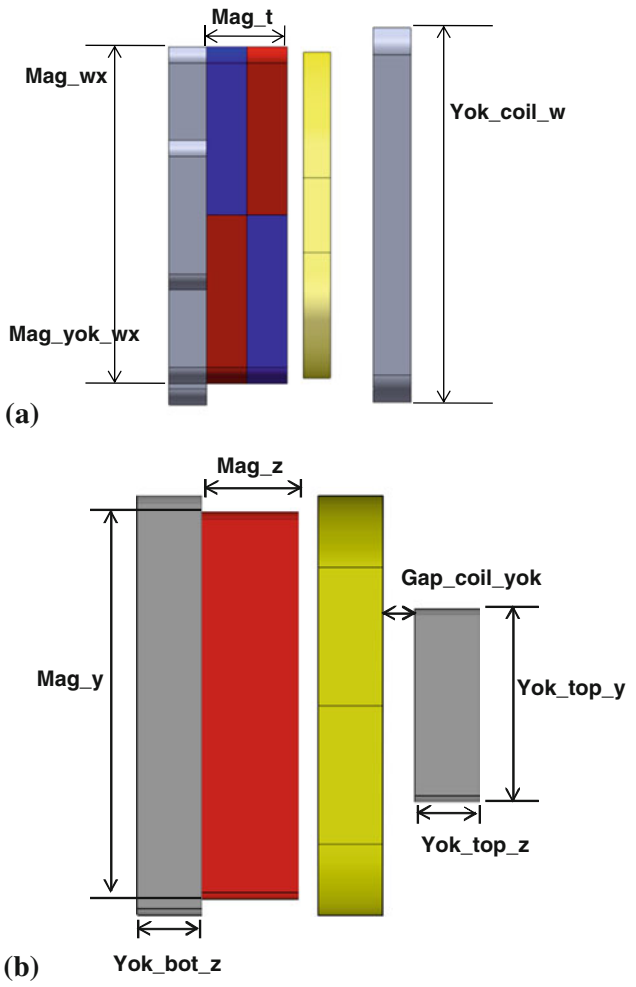

Fig. 9 Design variables **a** radial direction and **b** tangential direction

Table 5 Design variables for DOE in the radial direction

Variables (mm)	Item		
	Range	Step	Level
Mag_x	4.2–5.0	0.2	5
Yoke_coil_x	5.0–5.8	0.2	5
Yoke_mag_x	4.2–5.0	0.2	5
Mag_z	1.0–1.2	0.1	3

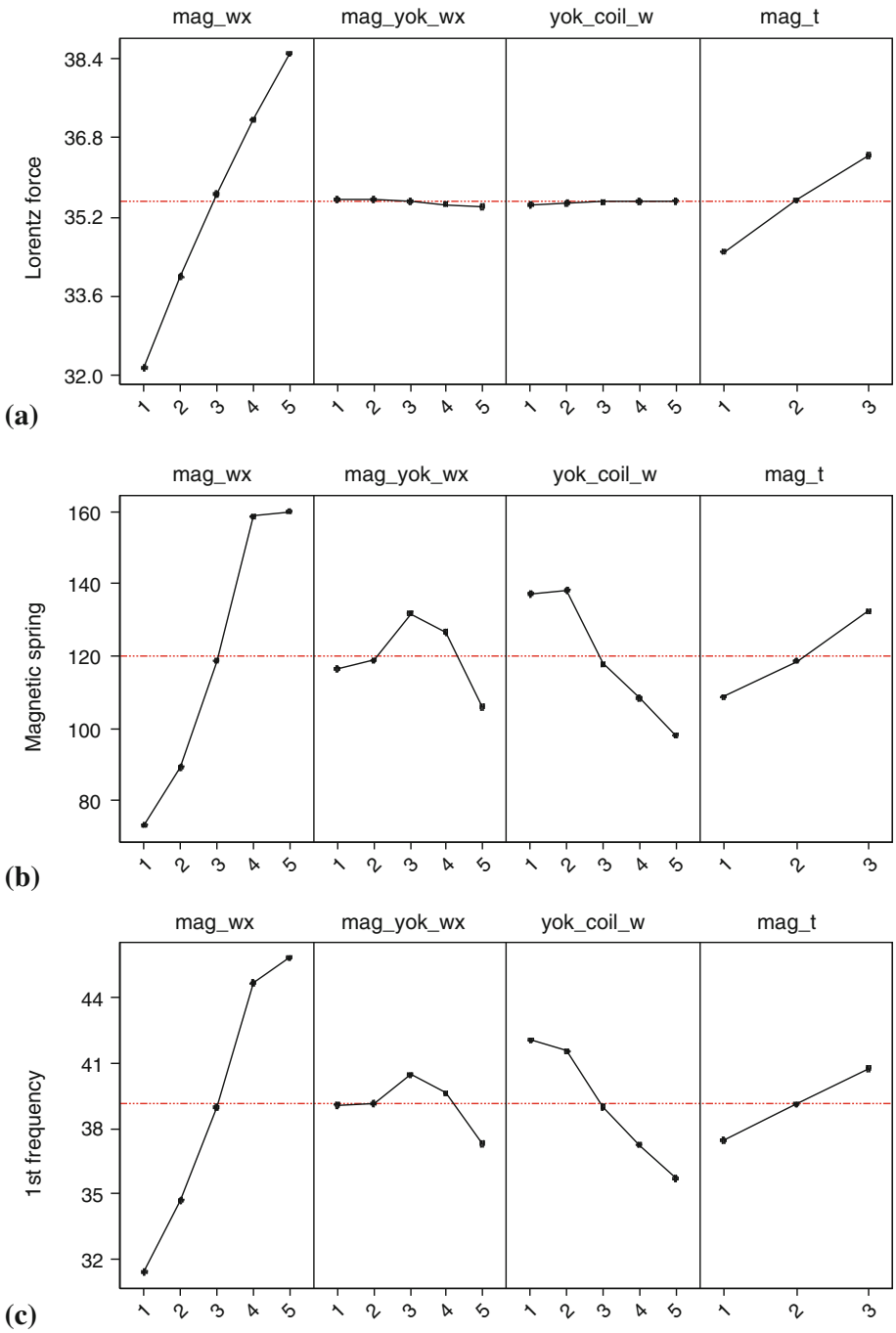

Fig. 10 Sensitivity analysis in the radial direction **a** Lorentz force, **b** magnetic spring and **c** first frequency

shows the design variables of the magnetic circuit that were used to perform the sensitivity analysis. The level of sensitivity analysis and range are shown in Table 6. As shown in Fig. 12, the size of magnet and the gap are very sensitive to the Lorentz force. The dynamic performance can be improved by selecting the sensitivity level for the design variables. Table 7 shows design values of optimized magnetic circuits for the radial and tangential directions.

4 Experimental results

Based on previous results, the final model was fabricated to verify its performance as shown in Fig. 13. Figure 14 shows the experimental setup for the dynamic tests of the fabricated actuator. A laser Doppler vibrometer (LDV) was used to obtain frequency responses. Figure 15 shows the frequency responses that were obtained from the experiments in each direction. The experimental

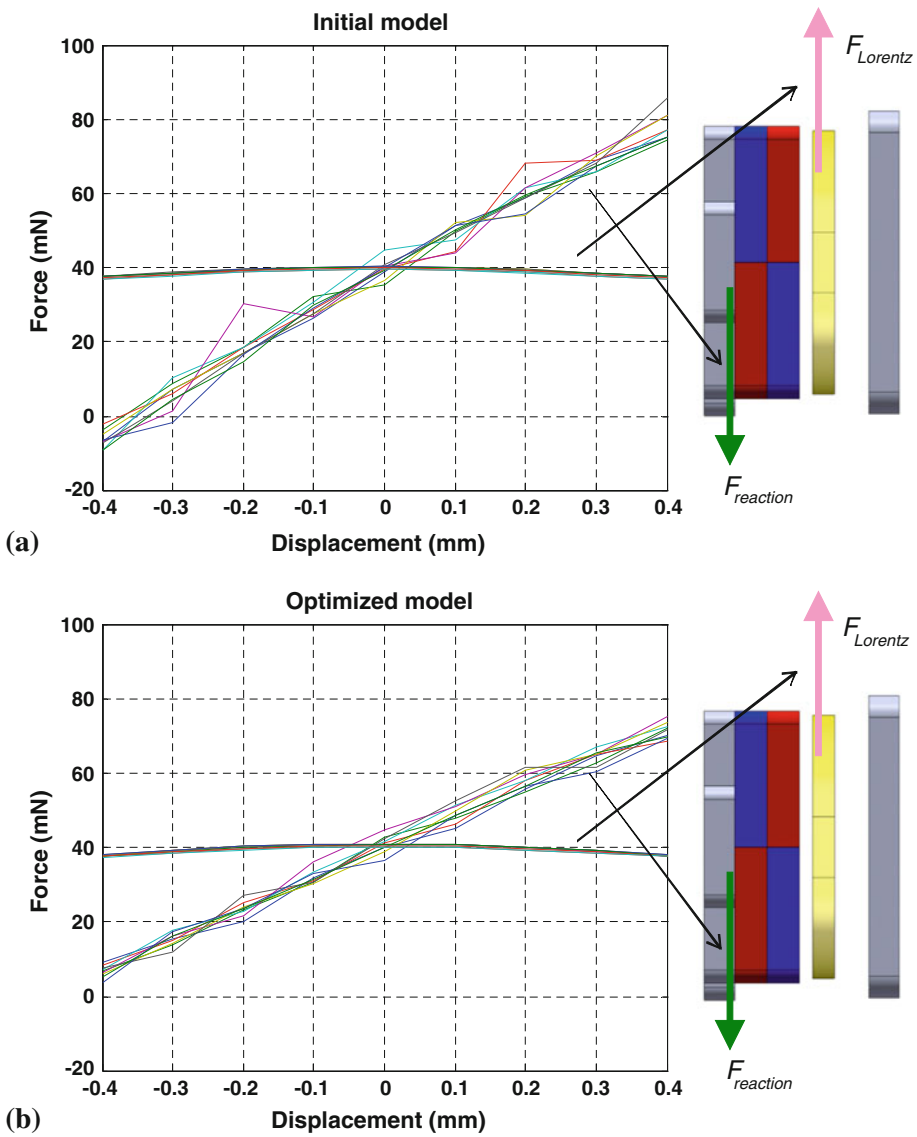

Fig. 11 Simulation results for the magnetic spring **a** initial model and **b** optimized model

Table 6 Design variables for DOE in the tangential direction

Variables (mm)	Item		
	Range	Step	Level
Mag_y	5.9–6.5	0.3	3
Mag_z	1.5–2.5	0.5	3
Gap_coil_yoke	0.5–0.9	0.2	3
Yoke_top_y	3.5–4.5	0.5	3
Yoke_top_z	1.0–2.0	1.0	2
Yoke_bot_z	1.0–2.0	1.0	2

responses were obtained with the LDV and a sine sweep signal. The AC sensitivities were 1.91 G/V in the radial direction and 2.17 G/V in the tangential direction. Table 8 shows a comparison of the optimized and experimental results for dynamic characteristics. As shown in Table 9, the performance of conventional actuator is compared with the one of the proposed actuator. Consequently, the high AC sensitivity of the actuator was verified for the radial and tangential directions when compared with the desired value. Therefore, the fabricated actuator exhibited satisfactory performance with the desired specifications.

5 Conclusions

A hybrid OIS actuator, which included a pivot bearing and ball guide, was proposed to compensate for hand trembling. Initially, the desired specifications of the OIS

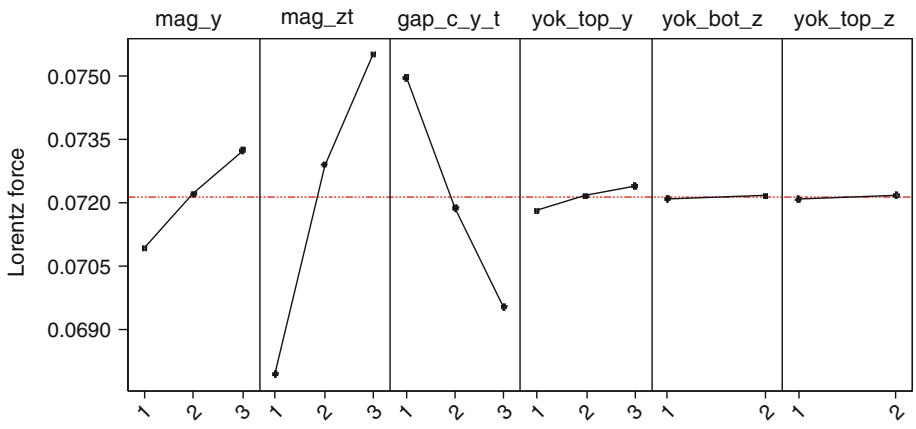

Fig. 12 Sensitivity analysis in the tangential direction

Table 7 Design values for the optimized magnetic circuit

Variables (mm)	Radial direction				Tangential direction			
	X	Y	Z	T	X	Y	Z	T
Magnet	4.2	6.0	1.0		18.4	5.3	1.5	
Yoke_mag	4.8	6.0	0.5		18.4	5.3	1.0	
Yoke_coil	5.8	6.0	0.5		26.0	3.0	1.0	
Coil	5.0	6.0	1.0	2.0	6.5	6.2	1.3	2.2

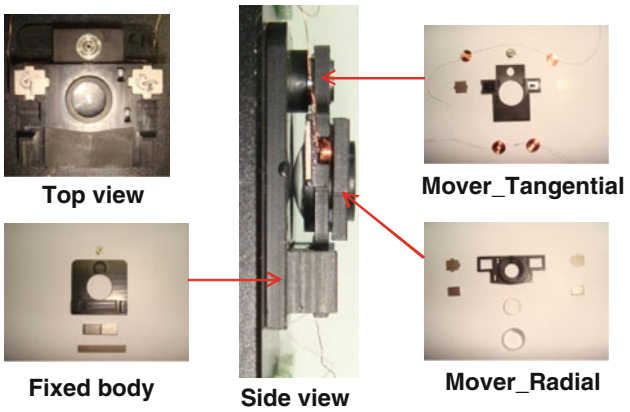

Fig. 13 Fabricated model

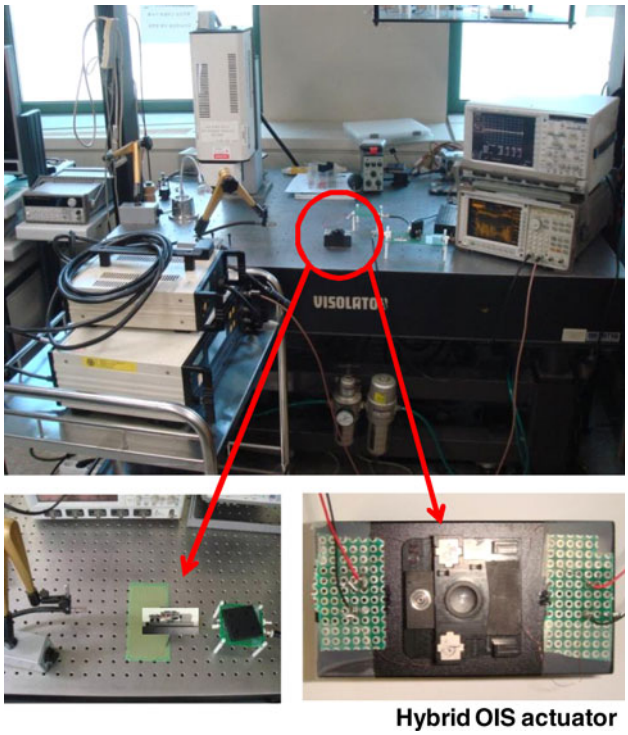

Fig. 14 Experimental setup

actuator were defined and the conceptual design was used for the driving mechanism and magnetic circuits. Two types of magnetic circuits were considered for the radial and tangential directions, and the linearity of the Hall-effect sensor was verified within the moving range. A sensitivity analysis was performed to improve the driving performance with the DOE procedure. Based on the sensitivity analysis, the objective function for the radial direction was defined by considering the constraints. Finally, the suggested OIS actuator for a digital camcorder was fabricated, and the feasibility of adapting two types of mechanisms was experimentally verified. In the future, an OIS system with the developed hybrid actuator will be fabricated, and its performance will be verified experimentally.

Table 8 Comparison of the optimized and experimental results

	Desired	Radial direction (MM type)		Tangential direction (MM type)	
		Optimized	Experiment	Optimized	Experiment
1st frequency (Hz)	30 ± 5	31.8	32	–	–
Magnetic spring (N/m)	65 ± 20	74.3	51.1	–	–
DC sensitivity (mm/V)	0.4	0.46	0.4	–	–
AC sensitivity (G/V)	1.2	1.95	1.91	2.44	2.17

Table 9 Comparison of the conventional and proposed actuator

	Desired	Radial direction (MM type)		Tangential direction (MM type)
		Conventional	Proposed	Proposed
1st frequency (Hz)	30 ± 5	31	32	–
DC sensitivity (mm/V)	0.4	0.1	0.4	–
AC sensitivity (G/V)	1.2	1.0	1.91	2.17

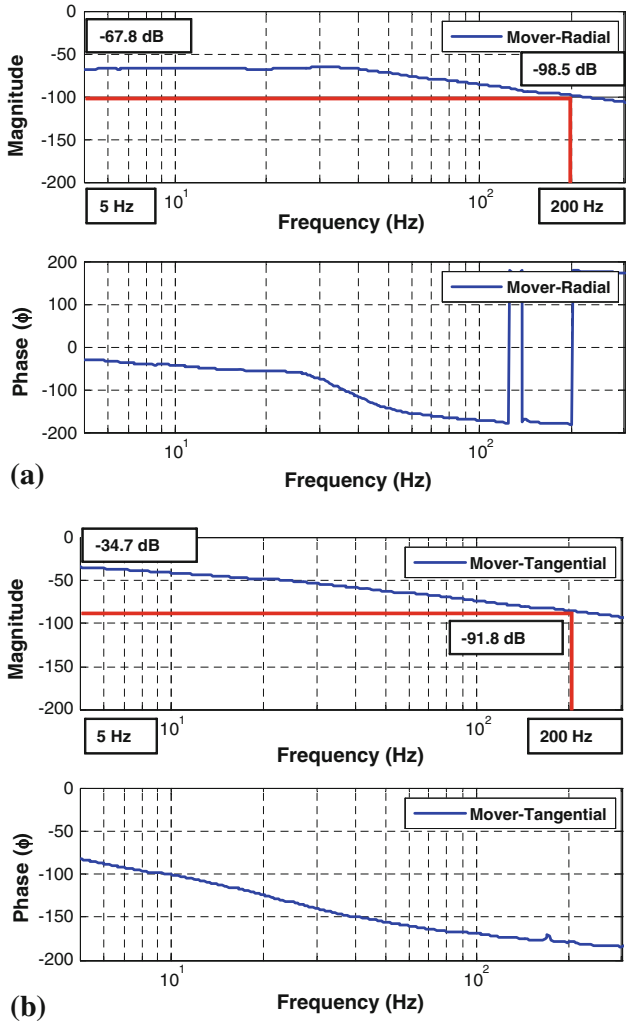

Fig. 15 Experimental results **a** FRF for radial direction and **b** FRF for tangential direction

Acknowledgments This work was supported by the National Research Foundation of Korea (NRF) grant funded by the Korea government (MEST) (No. 2010-0000769). In addition, the support of the SAMSUNG ELECTRONICS CO., LTD. is gratefully acknowledged.

References

Chiu CW, Chao PC-P, Wu DY (2007) Optimal design of magnetically actuated optical image stabilizer mechanism for cameras in mobile phones via genetic algorithm. IEEE Trans Magn 43(6):2582–2584

Choi H, Kim JP, Song MG, Kim WC, Park NC, Park YP, Park KS (2008) Effects of motion of an imaging system and optical image stabilizer on the modulation transfer function. Opt Express 16(25):21132–21141

Golik B (2006) Development of a test method for image stabilization systems. Diploma Thesis at the Cologne University of Applied Sciences

Kauhanen P, Rouvinen J (2006) Actuator for miniature optical image stabilizer. In: IEEE trans magnetics, 10th international conference on new actuators, pp 549–552

Ko SJ, Lee SH, Lee KH (1998) Digital image stabilizing algorithms based on bit-plane matching. IEEE Trans Consumer Electron 44(3):617–622

Koichi S, Shigeki I, Akira N, Mitsuru S (1993) Control techniques for optical image stabilizing system. IEEE Trans Consumer Electron 39(3):461–466

Song MG, Hur YJ, Park NC, Park YP, Park KS, Lim SC, Park JH (2009) Development of small sized actuator for optical image stabilization. IEEE Trans Magn 7:152–157

Song MG, Baek HW, Park NC, Park YP, Park KS, Lim SC (2010a) Development of small sized actuator with compliant mechanism for optical image stabilization. IEEE Trans Magn 46(6):2369–2371

Song MG, Son DH, Park NC, Park YP, Park KS, Lim SC (2010b) Design of ball bearing type OIS actuator for mobile camera module. KSNVE 20(4):361–372

Toshiro K, Naoki Y, Hiroyuki K, Satoshi T, Takuya I (1990) Electronic image stabilizer for video camera use. IEEE Trans Consumer Electron 36(3):520–525

Yu HC, Lee TY, Wang SJ, Lai ML, Ju JJ, Huang DR, Lin SK (2005) Design of a voice coil motor used in the focusing system of a digital video camera. IEEE Trans Magn 41(10):3979–3981